PHILOSOPHICAL TRANSACTIONS OF THE ROYAL SOCIETY A MATHEMATICAL, PHYSICAL & ENGINEERING SCIENCES

Diffuse Continental Deformation: Length Scales, Rates and Metamorphic Evolution

P. C. England

Phil. Trans. R. Soc. Lond. A 1987 **321**, 3-22
doi: 10.1098/rsta.1987.0001

Phil. Trans. R. Soc. Lond. A **321**, 3–22 (1987)

Printed in Great Britain

Diffuse continental deformation: length scales, rates and metamorphic evolution

By P. C. England†

Department of Geological Sciences, Harvard University, Cambridge, Massachusetts 02138, *U.S.A.*

In contrast with the oceanic portions of the plates, continents may deform hundreds of kilometres away from any plate boundary. Calculations that treat the continents as continuous media suggest that the across-strike length scale of deformation associated with a convergent boundary is proportional to the along-strike length of the boundary, the constant of proportionality depending on the rheology of the lithosphere. The dependence on convergent boundary length implies that, for fixed velocity of convergence, strain rates decrease with increasing length of the orogen. The dependence on rheology is less straightforward, but it appears from laboratory determination of flow laws that the scale length of compressional deformation decreases as the fraction of the lithospheric strength supported by friction on faults increases; that fraction depends on the thermal profile of the continental lithosphere and will change during the evolution of an orogenic belt. The thermal development of a diffusely deforming compressional belt is nearly independent of its strain history unless the strain rates are less than about 10^{-15} s^{-1}. If erosion terminates the heating phase of such an orogenic belt, the dominant control on the metamorphic history is the heat supply to the continental lithosphere. In contrast, if extension of the thickened crust ends metamorphism, peak metamorphic conditions depend only on the rheological properties of the lithosphere. Metamorphism in crust that is subject to major extension following compressional orogenesis should be nearly independent of the initial thermal conditions of the crust, and may be distinguished from metamorphism terminated by erosion by a final stage of isobaric cooling from temperatures close to the maximum experienced.

1. Introduction

An understanding of the controls on the length scales and rates of continental deformation is central to the study of the structural and metamorphic evolution of orogenic belts. It has been recognized since the first analyses of seismic activity in terms of the theory of plate tectonics that the deformation of the continents cannot be described as the relative motion of a few large rigid plates (Isacks *et al.* 1968). This difference in tectonic style is usually attributed to the greater buoyancy and lesser strength of the continental lithosphere (McKenzie 1969) but there is, as yet, no general agreement on a more specific characterization of the deformation.

Some interpretations of continental deformation postulate the existence of many small continental fragments that move separately from the larger plates but still (as they are presumed to move rigidly) obey the rules of plate tectonics (McKenzie 1972). In contrast, several authors have taken the view that the continents may be treated as continuous media (Molnar & Tapponnier 1975; Tapponnier & Molnar 1976; Bird & Piper 1980; England &

† Present address: Department of Earth Sciences, Oxford University, Parks Road, Oxford OX1 3PR, U.K.

McKenzie 1982, 1983; Vilotte *et al.* 1982, 1984; Houseman & England 1986*a*; England & Houseman 1986; Sonder *et al.* 1986*a*).

Support for each point of view may be found in observations of actively deforming zones. There are several aseismic and apparently undeforming regions in the Alpine–Himalayan belt, for example the Tarim Basin to the north-west of the Tibetan plateau (Molnar & Tapponnier 1981) and the regions of Central Turkey and Central Iran (Jackson & McKenzie 1984). Jackson and McKenzie suggest that the tectonics of part, at least, of the Alpine–Himalayan region is governed by rigid blocks, which are surrounded by deforming belts whose style of deformation (although more diffuse than that associated with inter-oceanic plate boundaries) may be predicted from the relative motion of the rigid blocks that bound them. An alternative view, investigated by Vilotte *et al.* (1984) and England & Houseman (1985) is that such regions are relatively strong inclusions within larger volumes of diffusely deforming continental lithosphere; in this case, although the motion of the stronger inclusion may still be described by rotation about a pole, that motion is governed by forces exerted on the inclusion by its surroundings and the scale lengths and rates of deformation are governed by the properties of the diffusely deforming regions of the continent.

The theory of plate tectonics is a kinematic one, therefore if continental deformation occurs by the relative motion of many small rigid fragments the lengthscales and rates for the deformation cannot be predicted, and must be found by determining the configuration of the rigid blocks in each region of interest. On the other hand, if the continents are effectively continuous it is possible to predict, at least approximately, the lengthscales and rates of deformation that result from a given boundary condition on the continental lithosphere. It has not yet been determined whether continental deformation is more accurately represented by the relative motion of many rigid plates or by the deformation of a continuum, and it may well be that each approach is useful, depending on the characteristics of individual deforming regions and on the scale at which they are observed.

This paper takes as its starting point the hypothesis that large scale continental deformation may be treated as a quasi-continuous process; its purpose is to outline the controls on the length scales and rates of deformation of such a continuous lithosphere and to relate these to the thermal and mechanical evolution of large compressional belts.

2. Deformation of a continuous continental lithosphere

2.1. *Scale lengths of compressional deformation*

In considering the deformation of continental lithosphere over many millions of years we may neglect accelerations, and the force balance equation reduces to the equation for creeping flow:

$$\partial\sigma_{i,j}/\partial x_j = \rho g a_i, \tag{1}$$

where $\sigma_{i,j}$ is the (i,j)th element of the stress tensor, ρ is the density of the medium, g is the acceleration due to gravity and $\boldsymbol{a}$ is the unit vector in the direction vertically downwards (z-direction). It is usual to neglect changes in volume during lithospheric deformation, so that

$$\nabla.\boldsymbol{u} = 0, \tag{2}$$

where $\boldsymbol{u}$ is the velocity. Equations (1) and (2), when combined with a constitutive equation

that relates strain rates to the stresses, yield four equations in four unknowns: the components of velocity and the pressure.

In studies of continental deformation these equations have usually been simplified either by assuming a state of plane strain ($u_z = 0$; Tapponnier & Molnar 1976) or by making the thin sheet approximation (Bird & Piper 1980; England & McKenzie 1983). The first of these simplifications involves no change in crustal thickness, so we shall concentrate on the thin sheet approximation, which perimits treatment of strain in the vertical direction, but yields only vertical averages of stress and strain. If we assume that the dimensions of any loads acting on the continental lithosphere are large in comparison with the thickness of the lithosphere and that shear stresses on the upper and lower surfaces of the lithosphere are negligible, then shear across horizontal planes may be neglected, only the vertical integrals of stress and strain rate need be considered, and solutions are expressed in terms of three variables: the horizontal components of velocity and the crustal thickness. Crustal thickness is specified as an initial condition and vertical strain rates (hence changes in crustal thickness) follow from (2) once the horizontal velocity is known (see Bird & Piper (1980) and England & McKenzie (1982) for discussion).

Full solution of the thin sheet equations requires numerical techniques, but it is possible to obtain approximate analytical solutions for the case in which the vertically integrated rheology of the thin sheet is taken to be a power law of the form

$$\tau_{i,j} = B\dot{E}^{(1/n-1)}\,\dot{\epsilon}_{i,j} \tag{3}$$

where $\tau_{i,j}$ is the (i,j)th component of the deviatoric stress tensor, $\dot{\epsilon}_{i,j}$ is the (i,j)th component of the strain rate tensor and $\dot{E}$ is the second invariant of the strain rate tensor:

$$\dot{E} = (\dot{\epsilon}_{i,j}\dot{\epsilon}_{i,j})^{\frac{1}{2}}. \tag{4}$$

It is observed from numerical experiments in which a normal or tangential velocity boundary condition is applied to part of the sheet (England & McKenzie 1983; Houseman & England 1986*b*; Sonder *et al.* 1986*a*) that, if the power law exponent, n, is greater than about 3, the velocities in the interior of the sheet are approximately parallel to those of the applied velocity condition. England *et al.* (1985) give approximate solutions to the thin sheet equations for the case when buoyancy forces due to crustal thickness contrasts within the sheet are negligible and the applied velocity condition is periodic with a wavelength of λ:

$$V = V_0 \cos(2\pi y/\lambda), \tag{5}$$

where V is the magnitude of the velocity applied normal or parallel to the y-axis of the region $x > 0$. The major component of velocity in the interior of the sheet is parallel to the boundary velocity given by (5) and its magnitude is approximately given by

$$V = V_0 \cos(2\pi y/\lambda)\,\mathrm{e}^{-x/l}, \tag{6}$$

where l is $\lambda/(4\pi\sqrt{n})$ if the velocity condition is parallel to the boundary and is $\lambda/(\pi\sqrt{n})$ for a velocity condition normal to the boundary.

Equation (6) implies that the strike-slip deformation associated with a transcurrent boundary should die out exponentially with distance away from the boundary with an e-folding length of $\lambda/(4\pi\sqrt{n})$ and that the compressional deformation associated with a convergent plate boundary should die out over a distance of $\lambda/(\pi\sqrt{n})$. England *et al.* (1985) and Houseman &

England (1986*b*) show that the solutions of (6) are also applicable to more geologically relevant boundary conditions, and suggest that a characteristic scale length for deformation associated with a continental convergence zone of along-strike length W is $2W/(\pi\sqrt{n})$, that the maximum compressional strain rate in the zone will be approximately $V_0\,\pi\sqrt{n}/(2W)$. The corresponding quantities for transcurrent deformation are $W/(2\pi\sqrt{n})$ and $2V_0\,\pi\sqrt{n}/W$. This feature might account for the observation that the width:length ratio of extensional or compressional zones in the continents (e.g. the Aegean, the Pannonian Basin, the Tibetan Plateau) is approximately $\frac{1}{2}$ to 1, whereas zones of predominantly transcurrent deformation (for example, southern California, Irian Jaya) are considerably narrower than they are long.

This paper concentrates on the results of convergent deformation; before applying the simple scaling relations given above we must determine the range of values of the power law exponent, n, that may be appropriate for the deformation of continental lithosphere.

2.2. *Vertically integrated rheology of continental lithosphere*

Brace & Kohlstedt (1980) summarize laboratory information on the stress required to deform the continental lithosphere at geological strain rates; they divide the lithosphere into three strata: the upper crust, which is assumed to fail by faulting and to obey Byerlee's law, the remainder of the crust, which is assumed to deform according to a steady state creep law for quartz, and the mantle, which is assumed to have the laboratory-determined properties of dry olivine that are summarized by Goetze (1978) (see table 1). The transition between failure by

TABLE 1. RHEOLOGICAL PARAMETERS FOR THE MODEL LITHOSPHERE

C	0, 60 MPa	Q	190, 510 kJ mol^{-1}
μ	0.85, 0.6	Q_D	536 kJ mol^{-1}
n	3	$\dot{\epsilon}_0$	5.6×10^{11} s^{-1}
R	8.314 J mol^{-1} K^{-1}	σ_0	8.5×10^3 MPa
B	5×10^{-6}, 7×10^4 MPa^{-3}		

The values of parameters are those given in Brace & Kohlstedt's (1980) summary of rheology of the lithosphere, except that the figure for the activation energy for creep of quartz has been corrected, and the activation energies for power law and Dorn law creep of olivine have been adjusted to give continuity of stress at the transition between them. In the crust the stress difference is the lesser of $\sigma_B = 2(c-\mu\sigma_{zz})/(1+\mu^2)^{\frac{1}{2}}-\mu)$ and $\sigma_P = (\dot{\epsilon}_{zz}/B)^{1/n}$ exp (Q/nRT). σ_B is an expression of Byerlee's law in the case of failure by thrust faulting, where σ_{zz} is the vertical stress and pore fluid pressure is assumed to be zero; C and μ take the first of the values given above when σ_{zz} is below 136 MPa and otherwise take the second values. σ_P is an expression for the stress difference in power law creep at a fixed strain rate; in the crust B and Q are assumed to take the values appropriate for quartz, which are the first values listed in the table, in the mantle, the second values (which are for olivine) are used. The stress difference in the mantle is given by the least of σ_B, σ_P and $\sigma_D = \sigma_0(1-(\ln(\dot{\epsilon}_0/\dot{\epsilon}_{zz})\,RT/Q_D)^{\frac{1}{2}})$ where σ_D is given by the Dorn plasticity law, which is assumed to operate at stress differences greater than 200 MPa. Density is taken to be 2.8 Mg m^{-3} throughout.

faulting and steady-state creep in the crust is chosen to occur at the level where the stresses required for operation of the two mechanisms are the same, and this level will be referred to as the brittle–plastic transition; below this depth the stress required to maintain deformation at a given strain rate falls off rapidly, owing to the strong temperature-dependence of the steady state creep of silicates. Note that this transition is a hypothetical one based on laboratory flow laws; it does not correspond to a seismic–aseismic transition, nor need it correspond to a 'brittle–ductile' transition defined on textural evidence from exhumed rocks (see also §4.2). The values of the rheological parameters used in this paper are given in table 1; they follow closely those of Brace & Kohlstedt.

PHILOSOPHICAL TRANSACTIONS OF THE ROYAL SOCIETY A MATHEMATICAL, PHYSICAL & ENGINEERING SCIENCES

In what follows there will be frequent mention of the relation between calculated stress and temperature distributions within the continental lithosphere. Brace & Kohlstedt do not discuss the uncertainties involved in extrapolating laboratory flow laws to geological strain rates, but there are, for example, considerable (more than 10%) variations in the reported activation energy for creep in olivine and very little quantitative is known about the mineral (or minerals) that govern the deformation properties of the crust. To avoid repetition, this uncertainty will not be referred to at every mention of temperature but it should be borne in mind that a 10% uncertainty in the activation energy for creep is equivalent to a 10% uncertainty in the absolute temperature for a given stress, or to a threefold to tenfold uncertainty in stress for a given strain rate and temperature.

Sonder & England (1986) have calculated vertical integrals of the stress required to deform a thin sheet (§2.1) of continental lithosphere obeying the rheology summarized above, and show that, over a wide range of strain rate and thermal conditions, the relation between the strain rate and the vertically integrated stress required to maintain that strain rate is approximately given by (3). Values for the power law exponent, n, considerably higher than three (the value that would be appropriate for the steady creep of silicates, e.g. table 1) result from the inclusion within the vertically integrated rheology of high stress plasticity (Goetze 1978) and of strain rate-independent failure by sliding on faults.

Figure 1 shows the dependence of power law exponent, n, on Moho temperature for a range of conditions influencing the contribution of the brittle upper crust to the integrated rheology. The higher the fraction of the integrated stress that is supported by friction on faults, the higher is the effective power law exponent. Most of the conditions illustrated yield values of n between 3 and 20, although values of n greater than 20 are reached with Moho temperatures below 400 and above 700 °C, as well as for the curve with the brittle–plastic transition at 20 km. The effective power law exponent calculated from the stress–strain rate relations of the model lithosphere described in this paper (see §3.1) varies from about 8 when the surface heat flux is 70 mW m^{-2} to about 11 for the case in which it is 40 mW m^{-2}.

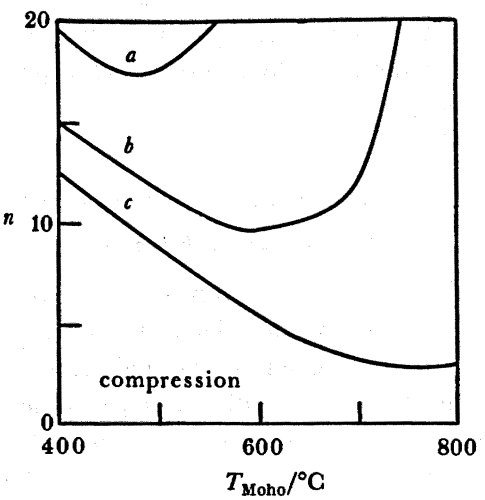

FIGURE 1. (After Sonder & England (1986).) Dependence of effective stress exponent (n, equation 3) on the temperature at the Moho for continental lithosphere with the brittle–plastic transition at 20 km (curve a) and 10 km (curve b), and pore fluid pressure equal to zero. Curve c shows the value of effective stress exponent calculated by neglecting the crustal contribution to lithospheric strength. See Sonder & England (1986) for details of calculation.

PHILOSOPHICAL TRANSACTIONS OF THE ROYAL SOCIETY A MATHEMATICAL, PHYSICAL & ENGINEERING SCIENCES

Equation (6) shows that compressional deformation will be spread out over an across-strike width of 0.1 ($n = 30$), 0.2 ($n = 10$) or 0.4 ($n = 3$) of the along-strike length of the boundary. Table 2 lists the values of compressional scale length, l, and maximum compressional strain rate, $\dot{\epsilon}_{zz}$, that are calculated from (6) for a range of compressional boundary lengths and n. Strain rates higher than 10^{-14} s^{-1} are associated with values of n above 10, and with convergent boundary length less than 300 km; under these conditions the lengthscale of convergent deformation is less than the lithosphere thickness.

TABLE 2. LENGTH SCALES AND STRAIN RATES FOR DISTRIBUTED COMPRESSIONAL DEFORMATION

	$n = 3$		$n = 10$		$n = 30$	
	l/km	$\dot{\epsilon}_{zz}$/s^{-1}	l/km	$\dot{\epsilon}_{zz}$/s^{-1}	l/km	$\dot{\epsilon}_{zz}$/s^{-1}
W, 300 km	110	—	60	—	35	—
W, 1000 km	370	3×10^{-15}	200	5×10^{-15}	120	—
W, 3000 km	1100	9×10^{-16}	600	2×10^{-15}	350	3×10^{-15}

Scale lengths, l, and maximum compressional strain rates, $\dot{\epsilon}_{zz}$, calculated from equation (6) for different values of n (equation 3) and compressional boundary length, W. $\dot{\epsilon}_{zz}$ is calculated assuming a convergent velocity V_0 (equation 6) of 30 mm a^{-1}, and is not shown for values of l less than 200 km, as distributed deformation is not expected to be described by equation (6) under these conditions (see text).

It should be emphasized that the scale lengths determined in this section take no account of the buoyancy forces associated with crustal thickness contrasts that result from the compressional strain. These forces have the effect of limiting the total crustal thickening that may occur, and thus of increasing the scale length of the compressional deformation (see Molnar & Tapponnier 1975; Tapponnier & Molnar 1976; England & McKenzie 1983; Houseman & England 1986*b*).

There is a range of conditions ($n \lesssim 10$; $W \gtrsim 1000$ km) under which the deformation is spread out over a horizontal length scale considerably greater than the lithospheric thickness. The corresponding strain rates, assuming convergent velocities between 10 and 100 mm a^{-1}, lie between 3×10^{-16} s^{-1} and 10^{-14} s^{-1} (see table 2). The calculations of the following section will be made with this range of strain rates (which is that, according to this continuum approach to continental deformation, in which diffuse deformation is expected to occur in zones of continental convergence).

3. THERMAL AND MECHANICAL DEVELOPMENT OF COMPRESSIONAL TERRAINS

3.1. *The model lithosphere*

Calculations of thermal profiles and mechanical properties of the lithosphere are carried out with the rheological parameters having values given in table 1 and the thermal parameters having the values given in table 3. The initial thermal structure is that of a continental lithosphere whose geotherm is in steady state with a surface temperature of 0 °C and a surface heat flow Q_0, half of which is generated uniformly throughout the upper 16 km of the crust; the lithosphere has a thickness of 128 km and the crust is 35 km thick. The thermal diffusivity and thermal conductivity of the lithosphere are 9×10^{-7} m^2 s^{-1} and 2.25 W m^{-1} K^{-1}, respectively. These are values chosen to be representative of properties of the crust, where most of the temperature changes that will concern us occur, it is probable that the conductivity of the

Table 3. Thermal parameters for the model lithosphere

lithosphere thickness, a	128 km
thermal diffusivity, κ	9×10^{-7} m^2 s^{-1}
thermal conductivity, K	2.25 W m^{-1} K^{-1}
crustal thickness	35 km
undisturbed surface heat flux, Q_0	40, 50, 60, 70 mW m^{-2}
rate of heat production, A, from surface to depth D (16 km)	1.25, 1.56, 1.875, 2.19 μW m^{-3}

upper mantle is greater than 3 W m^{-1} K^{-1}, so that the mantle thermal gradients calculated in this paper are steeper than would be found in the lithosphere under similar conditions.

As the heavy temperature dependence of the strength of silicates is the dominant effect in the development of the mechanical structure of the lithosphere during deformation, the most important parameters to vary are those that affect the thermal profile. For simplicity this is done by varying the initial surface heat flux, leaving the proportion (one half) of the heat flux that is generated in the crust, and the other parameters in table 3, unchanged. Values of the initial surface heat flux between 40 and 70 mW m^{-2} are used in the calculations.

The lithosphere is perturbed from its initial thermal profile by homogeneous biaxial strain, with one axis vertical, at a prescribed rate; the temperatures at 0 and 128 km are kept at the values calculated for the reference state and temperatures are calculated by a standard finite difference technique (see Houseman & England 1986*a* for details). At any time, the force per unit length (equation (8)) required to deform the lithosphere may be calculated by numerical integration of the stress as a function of depth, and the depth of brittle–plastic transition may be determined by finding the depth at which the quartz flow law and Byerlee's law give the same deviatoric stress (table 1).

3.2. *Thermal and mechanical evolution during compression*

All strain rates used in this section are assumed to be independent of time, so for a given strain rate, $\dot{\epsilon}_{zz}$, the compressional strain γ, at any time, t is

$$\gamma = e^{\dot{\epsilon}_{zz} t}. \tag{7}$$

The results in this section are from calculations in which the model lithosphere of §3.1 is thickened at strain rates of 3×10^{-16} s^{-1} to 10^{-14} s^{-1} up to a maximum compressional strain of $\gamma = 2$.

3.2.1. *Moho temperatures*

The variation in temperature at the Moho is an indicator of the temperature change throughout the crust during deformation; this will be discussed further below (§3.3), where pressure–temperature paths are presented for rocks buried at different levels within the lithosphere. In addition, the strength of the mantle portion of the lithosphere depends greatly on the temperatures in the uppermost mantle. Figure 2 shows the Moho temperature plotted against compressional strain for strain rates of 3×10^{-16} and 10^{-15} s^{-1} and for thermal conditions defined by surface heat fluxes of 40 to 70 mW m^{-2}. At 3×10^{-16} s^{-1}, 100% strain takes over 70 Ma, which is more than the thermal time constant of the lithosphere, and temperature changes of between 70 and 125 °C occur at the Moho. In contrast, there is only a 10 to 15 °C temperature rise in the curves corresponding to the strain rate of 10^{-15} s^{-1}; higher

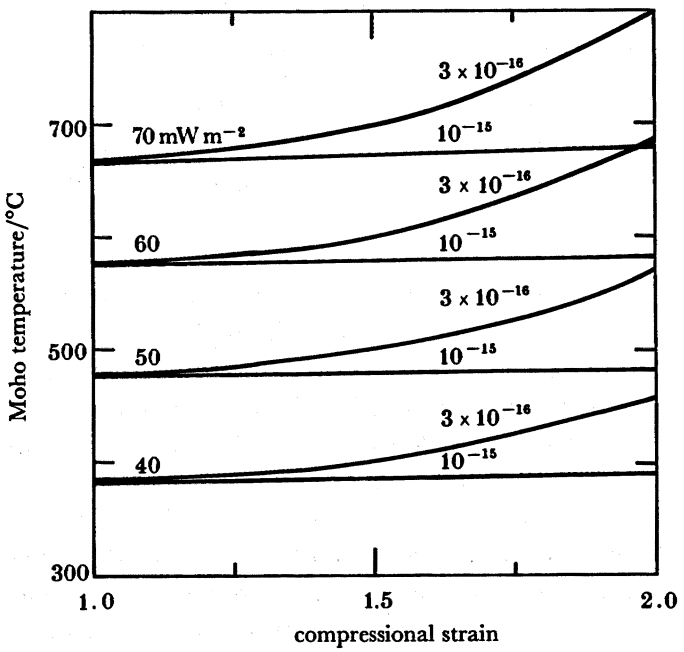

FIGURE 2. Moho temperature plotted against compressional strain (γ, equation 7) for different geotherms that are characterized by the surface heat flows given by the curves (see table 3). The strain rate, in reciprocal seconds, is given by each curve.

strain rates are not illustrated because, provided that the strain rate exceeds 10^{-15} s^{-1} (less than 20 Ma for 100% strain), the deformation occurs practically isothermally in the lower crust and upper mantle.

3.2.2. *Lithospheric strength*

The force per unit length (equation (8)) necessary to sustain the deformation of the lithosphere is

$$F_L = \int_0^a (\sigma_1 - \sigma_3)\, dz, \tag{8}$$

where the differential stress $(\sigma_1 - \sigma_3)$ is evaluated according to the relations in table 1. If F_L is divided by the lithospheric thickness and by the strain rate for the particular calculation it gives a quantity that may be thought of as the vertically averaged effective viscosity of the lithosphere. F_L represents only the force required to deform the material of the lithosphere; there is also a force required to support thickened, isostatically compensated continental crust. This force is proportional to the difference between the squares of the crustal thicknesses before and after thickening and, for example, the force per unit length necessary to support the elevation contrast of 5 km represented by the Tibetan plateau is approximately 6×10^{12} N m^{-1} (Frank 1972).

Figure 3*a* shows the variation in F_L with strain for the calculations with Q_0 equal to 60 mW m^{-2}; note that there is an uncertainty of at least a factor of ten in the absolute magnitude of these stresses (§2.2) and that the force required to support the thickened crust, which is not subject to the same degree of uncertainty, is not included. The force that must be provided externally to do work deforming the lithosphere increases during the deformation, except at

the strain rate of 3×10^{-16} s^{-1}. The force doubles at a strain rate of 10^{-14} s^{-1}, but the increase is not proportional to the strain at the lower strain rates, because even a few tens of degrees' temperature rise at the Moho can lower the driving stress appreciably (see also England 1983*a*) and because the brittle–plastic transition does not migrate proportionally to the strain (see §3.2.3).

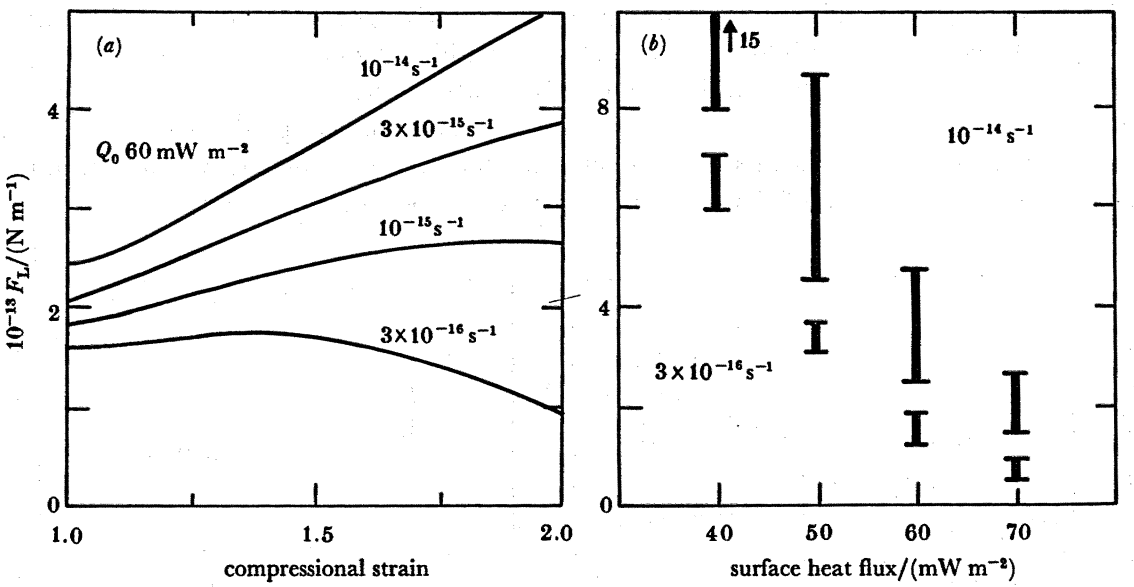

FIGURE 3. (*a*) The force, per unit length of continental lithosphere, required to sustain deformation at a specified strain rate (F_L, equation 8) for calculations in which the undisturbed surface heat flux is 60 mW m^{-2}. Compressional strain rates are shown by each curve. (*b*) Range in F_L during a compressional strain of 100% at strain rates of 10^{-14} s^{-1} (upper bars) and 3×10^{-16} s^{-1} (lower bars), for calculations with surface heat flux 40, 50, 60 and 70 mW m^{-2}.

These changes may be expected to influence the configuration of deformation within the compressional zone because the vertically integrated effective rheology of the lithosphere will change during the deformation. In particular, the effective viscosity of the more slowly deforming regions will tend to decrease with time, whereas it will increase in the more rapidly deforming regions; this should be contrasted with the behaviour of a temperature-independent power law fluid, in which the effective viscosity is inversely dependent on the strain rate.

Similar behaviour is observed for the values of driving force per unit length calculated with the other surface heat flows; these are summarized in figure 3*b*, which shows the range of F_L calculated for each thermal profile at strain rates of 3×10^{-16} s^{-1} and 10^{-14} s^{-1}. In each case the integrated stress increases approximately two-fold during the deformation at the higher strain rate, and increases slightly, then decreases, at the lower strain rates. Note that the increase in integrated stress (or effective viscosity) during compression at 10^{-14} s^{-1} is approximately equivalent to the difference produced by a 10 mW m^{-2} decrease in surface heat flow (*ca.* 100 °C change in Moho temperature; see figure 2). Consequently, pre-deformational lateral heterogeneities in strength, if they are caused by lateral variations in thermal structure, as suggested by Molnar & Tapponnier (1981) for the Tarim Basin in Central Asia, are of comparable importance to lateral variations in strength produced during the deformation.

3.2.3. *Brittle–plastic transition*

Figure 4*a* shows the variation in the depth to the brittle–plastic transition (determined as described in §3.1) during calculations with initial surface heat flows of 40 and 70 mW m^{-2} at strain rates of 10^{-14} to 3×10^{-16} s^{-1}. As in the case of the vertically integrated stress, the temperature rise that accompanies compressional deformation at the lowest strain rates is sufficient to keep the brittle–plastic transition close to its original depth. Unlike the integrated stress, F_L, however, the depth to the brittle–plastic transition does not increase proportionally to the strain even at the highest strain rates considered. In all the cases illustrated in figure 4*a*, the initial position of the brittle–plastic transition is within the heat-producing layer (§3.1); the heat generation provides a temperature change that is felt immediately, in contrast to the temperature rise owing to diffusive thermal relaxation of the whole lithosphere.

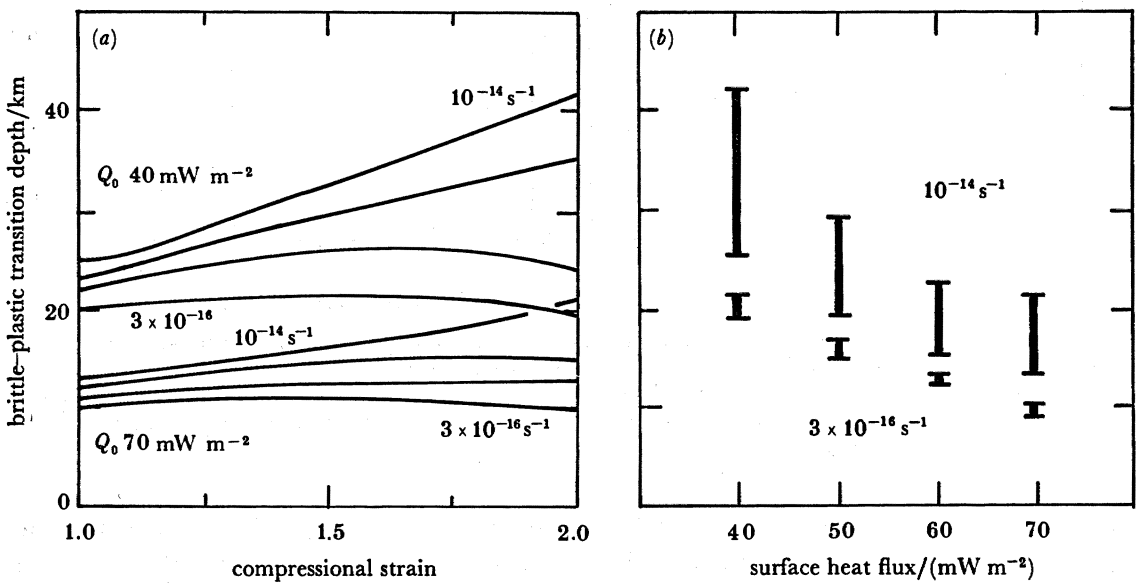

FIGURE 4. Depth of brittle–plastic transition during a compressional strain of $\gamma = 2$ (equation 7) calculated using rheological parameters of table 3. (*a*) Undisturbed surface heat flux is 40 and 70 mW m^{-2} and strain rates are 3×10^{-16} to 10^{-14} s^{-1}. (*b*) Undisturbed surface heat flux is 40, 50, 60 or 70 mW m^{-2}, upper bars show range of depths of brittle–ductile transition at a strain rate of 10^{-14} s^{-1} from $\gamma = 1$ to $\gamma = 2$ and lower bars are for a strain rate of 3×10^{-16} s^{-1}. (See also figure 7.)

The transfer of heat in a medium of constant thermal diffusivity, thermal conductivity and heat production, in which temperature depends only on the coordinate z is described by

$$\frac{\partial T}{\partial t} = \kappa \frac{\partial^2 T}{\partial z^2} - u_z(z) \frac{\partial T}{\partial z} + \frac{A\kappa}{K}, \tag{9}$$

where T is temperature, z is depth, A is the rate of heat production, u_z is the vertical velocity and the other symbols are defined in table 3. In order for the internal heat generation to be able to keep the brittle–plastic transition at, or above, its original depth during deformation, the right-hand side of (9) must be greater than, or equal to, zero. Consider a régime in which a strain of γ has occurred with very little thermal diffusion: all the gradients of temperature

will have $1/\gamma$ times their initial value and we may make use of the fact that, before deformation begins, the first and third terms in the right-hand side of (9) are equal and opposite. In these calculations we have assumed that the crustal contribution is half the surface heat flow ($AD = \frac{1}{2}Q_0$) and we may estimate $\mathrm{d}T/\mathrm{d}x$ to be approximately $Q_0/(2\gamma K)$, so that we may approximate the right-hand side of (9) by

$$(\kappa A/K)\,(1-1/\gamma^2) - u_z(z)\,AD/K\gamma. \tag{10}$$

Equation (10) leads to the requirement for the increase in temperature at a particular level owing to heat generation to be greater than the decrease owing to the downward advection of cold material

$$\dot{\epsilon}_{zz} = \frac{u_z(z_t)}{z_t} \lesssim \frac{\kappa\gamma\,(1-1/\gamma^2)}{Dz_t} \approx \frac{\kappa}{D^2} \approx \frac{\kappa}{z_t^2}, \tag{11}$$

where z_t is the depth of the level of interest; in this case the brittle–plastic transition. Substituting values of the parameters obtained from table 3 and figure 4 for the case in which the vertical strain, γ, is equal to 2 gives the approximate result that, if the strain rate is less than about 3×10^{-15} to 6×10^{-15} s^{-1}, the rate of heat production within the upper crust will be great enough to prevent the downward migration of the brittle–plastic transition. The calculations of figure 4*a* show that the critical strain rate is between 1×10^{-15} and 3×10^{-15} s^{-1} when Q_0 is 40 mW m^{-2}, and between 3×10^{-15} and 10^{-14} s^{-1} when Q_0 is 70 mW m^{-2}.

3.3. *Metamorphic evolution of broad orogenic belts*

Previous calculations of thermal regimes resulting from continental thickening have commonly assumed that the agency terminating metamorphism is erosion acting on the elevated surface of the thickened crust (see, for example, Albarede 1976; Richardson & Powell 1976; England & Richardson 1977; England & Thompson 1984). If this is so, and if the compressional belt is assembled in less than the thermal time constant of the lithosphere, then the discussion above indicates that the thermal evolution of such an orogenic belt will be virtually independent of the duration of its compressional history; figure 2 indicates that there is little temperature rise within the crust during compressional deformation as long as the strain rate is more than 10^{-15} s^{-1}. Under these conditions, the primary controls on the intensity of metamorphism are the magnitude of the thermal perturbation introduced by the thickening of the lithosphere and the length of time that is available for this thermal perturbation to decay before erosion stops the heating of a particular level in the crust. England & Thompson (1984) show, for example, that if the crust of a lithosphere thickened as described above is returned to its original thickness by erosion acting over 100 Ma, the maximum temperature experienced at the base of the crust varies from about 460 °C if the undisturbed surface heat flow, Q_0, is 45 mW m^{-2}, to 830 °C if Q_0 is 75 mW m^{-2}; greater variation occurs if the average thermal conductivity of the lithosphere is varied, and the extremes of Moho temperature calculated by England & Thompson for this case are 360 and 1200 °C (England & Thompson 1984, figure 5*c*, *g*).

In this paper we are primarily discussing the evolution of broad compressional belts, such as the Tibetan Plateau at present or Western North America in the late Mesozoic and early Tertiary. Although considerable erosion occurs on the edge of the Tibetan plateau, there is little precipitation in the interior, and most of the erosion that occurs there appears to be into internal basins. It seems likely that the extension already occurring in Tibet (Molnar &

Tapponnier 1975, 1978; Tapponnier & Molnar, 1976) will terminate the heating of this belt; this was probably also the case for much of the Mesozoic compressional belt of western North America (Molnar & Chen 1983; Coney & Harms 1984; Sonder *et al.* 1986). This section explores some of the probable consequences of such a tectonic history.

3.3.1. *Timing of post-compressional extension*

Figure 3 shows the force per unit length necessary to sustain the deformation of the continental lithosphere under a variety of conditions. As discussed above (and by England & Houseman 1986) this force may be considerably greater than that necessary to support the topography alone; its magnitude is determined by the boundary conditions applied to the continental lithosphere, and the requirement for deformation to continue is that a sufficient driving force is available from the system of forces driving plate motion as a whole.

In contrast, the forces driving extension of the continental lithosphere are simply those due to its potential energy contrast with its surroundings (Tapponnier & Molnar 1976; Molnar & Lyon-Caen 1986); consequently the extensional strain rate immediately after the end of thickening may be a small fraction of the compressional strain rate during thickening. Sonder *et al.* (1986*b*) discuss the mechanical evolution of compressional belts using rheological parameters similar to those employed here and provide a rule-of-thumb for defining the condition necessary for appreciable extension to begin; this is that the Moho temperature should exceed approximately 750 °C. The basis for the rule-of-thumb is as follows. The extensional driving forces arising from isostatically-compensated elevation contrasts within the continents are a few times 10^{12} N m^{-1} (perhaps 8×10^{12} N m^{-1} in the case of the Tibetan plateau (Frank 1972; Molnar & Lyon-Caen 1986) to 2×10^{12} N m^{-1} in the case of the Aegean Sea (Le Pichon 1983)) and this discussion takes 4×10^{12} N m^{-1} as a representative value for these driving forces. The parameter that most strongly influences the strength of the lithosphere (and so the rate at which it will strain in response to the forces) is the temperature at the Moho. In figure 5, the calculations described so far (figures 2–4) are continued after the compressional deformation ends, and the geotherm at any time is characterized by its Moho temperature; the hatched band contains the strain rates, calculated for that geothermal profile, that would result from an extensional force of 4×10^{12} N m^{-1} applied to the rheologically layered lithosphere considered here. The right-hand edge of the band corresponds to strain rates for calculations in which the undisturbed surface heat flow, Q_0, is 70 mW m^{-2}, and the left-hand edge to the case in which Q_0 is 40 mW m^{-2}. If the Moho temperature is less than 675 °C none of the calculated strain rates exceeds 10^{-16} s^{-1} (100% extension in 200 Ma), while if the Moho temperature exceeds 790 °C no calculated strain rate is less than 10^{-15} s^{-1} (100% extension in 20 Ma). Figure 5 also shows the range of Moho temperatures over which driving stresses of 2, 6 and 8×10^{12} N m^{-1} result in extensional strain rates of 10^{-15} s^{-1}.

There is clearly a set of conditions (corresponding, in the case considered here, to geotherms with initial surface heat fluxes below 50–40 mW m^{-2}, see figures 6 and 7) in which the Moho temperature fails to reach the temperature necessary for appreciable extensional strain to occur. There is also a narrower range within which extensional strain might occur at a rate rather less than 10^{-15} s^{-1}. The calculations below are primarily intended to illustrate the kind of metamorphic history to be expected in a terrain that is subjected to rapid extension after compression; for simplicity it is assumed that extension of the thickened continental lithosphere begins at a rate of 10^{-15} s^{-1} immediately that the Moho temperature reaches 750 °C. The

PHILOSOPHICAL TRANSACTIONS OF THE ROYAL SOCIETY A MATHEMATICAL, PHYSICAL & ENGINEERING SCIENCES

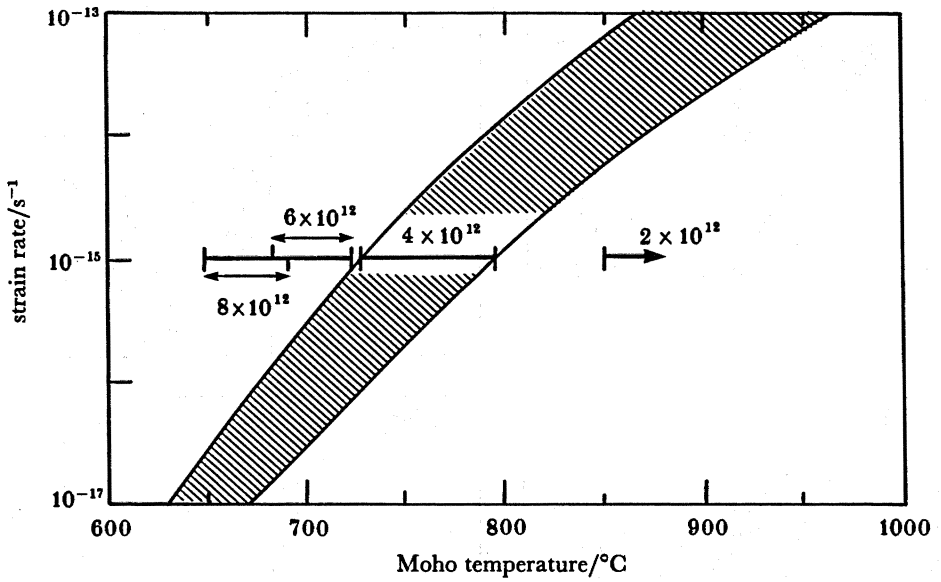

FIGURE 5. Geothermal profiles are calculated for the sixteen combinations of Q_0 (40, 50, 60 and 70 mW m^{-2}) and compressional strain rate (3×10^{-16}, 1 and 3×10^{-15} and 10^{-14} s^{-1}), with no strain occurring after the end of compression; the geotherm at any time is represented in the figure by its Moho temperature. Notional strain rates plotted are those that would result from the application of vertically integrated extensional deviatoric stress of 2, 4, 6, or 8×10^{12} N m^{-1} to the lithosphere. The hatched band contains all the solutions for an extensional force per unit length of 4×10^{12} N m^{-1}. The symbols at a strain rate of 10^{-15} s^{-1} show the range of Moho temperatures that give rise to this strain rate if forces of 8, 6 and 2×10^{12} N m^{-1} were applied to the lithosphere.

reader is referred to Sonder *et al.* (1986*b*) for a more detailed treatment of the mechanical development of such a lithosphere, that takes account of the changes in potential energy and strength of the lithosphere during its extension.

3.3.2. *Pressure–temperature paths for extending orogenic belts*

The principal feature of the metamorphic histories calculated under the assumption that lithospheric extension, rather than erosion, is responsible for terminating the metamorphism is that, owing to the heavy dependence on temperature of the strength of the lithosphere, the onset of extension, and consequent cooling of the crust, is expected to occur over a relatively narrow range of thermal conditions, irrespective of the thermal conditions before, or at the end of, the compression that formed the orogenic belt.

Figure 6 shows the pressure–temperature paths of rocks in a continental crust that is first subjected to thickening by a factor or two, and is subsequently thinned by the same factor, extension occurring at a rate of 10^{-15} s^{-1} once the Moho temperature exceeds 750 °C. Figure 6*a*, *b* shows calculations in which the undisturbed surface heat flux, Q_0, is 60 mW m^{-2} and the compressional strain rate is 10^{-14} s^{-1} (figure 6*a*) and 3×10^{-16} s^{-1} (figure 6*b*); the pressure–temperature paths for each case are very similar once extension begins, and the principal difference between the two cases is that the interval between the end of compression and the onset of extension is 30 Ma in figure 6*a* and 10 Ma in figure 6*b*. Figure 6*c*, *d* shows pressure–temperature paths for two calculations in which the compressional strain rate is 10^{-15} s^{-1} and the value of Q_0 is 50 mW m^{-2} (figure 6*c*) and 70 mW m^{-2} (figure 6*d*). The pressure–temperature paths in the exhumation phase differ between these two cases, with the

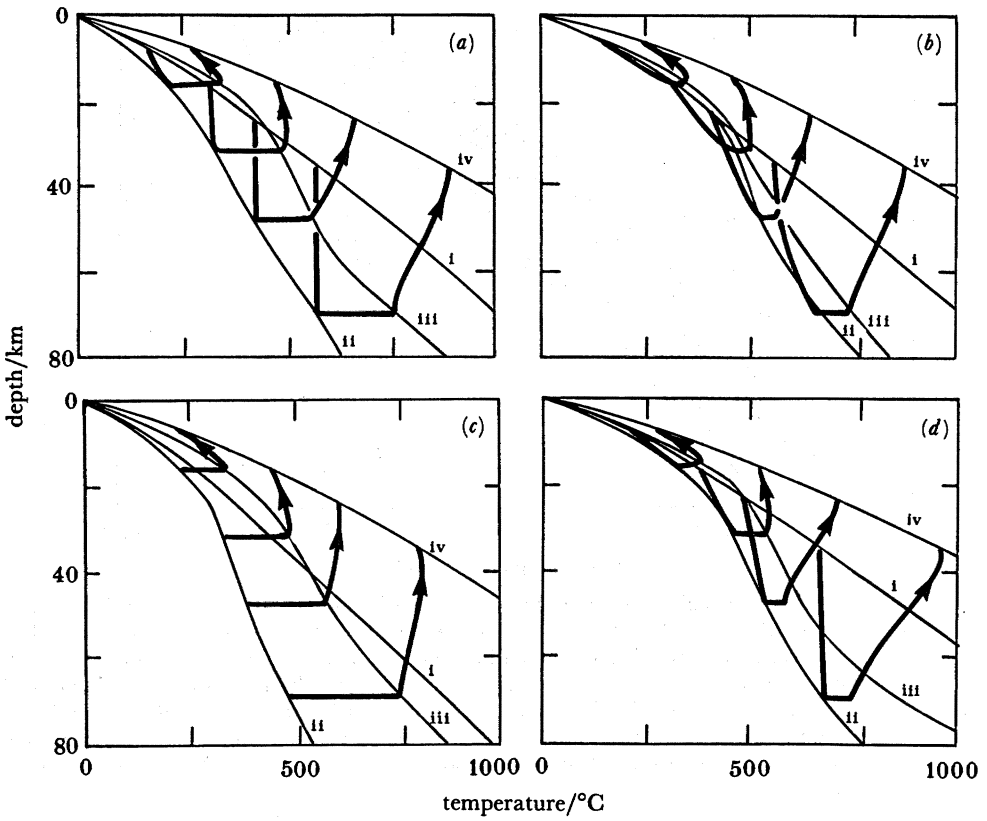

FIGURE 6. Geotherms (thin lines), and pressure–temperature paths (thick lines) calculated for rocks initially at 7.5, 15, 22.5 and 35 km in continental lithosphere of thermal parameters given in table 3. Geotherms (i), (ii), (iii), (iv) correspond to times: (i) immediately before compression; (ii) at the end of compression; (iii) at the onset of extension, taken to be the time when the Moho reaches a temperature of 750 °C (see text); (iv) at the end of extension. In each case there is compressional strain (thickening) by a factor of two and an equal amount of extensional strain (that occurs at 10^{-15} s^{-1}), so that the initial and final crustal thicknesses are the same.

(*a*) Compressional strain rate, 10^{-14} s^{-1}; Q_0 60 mW m^{-2}. (*b*) Compressional strain rate, 3×10^{-16} s^{-1}; Q_0 60 mW m^{-2}. (*c*) Compressional strain rate, 10^{-15} s^{-1}; Q_0 50 mW m^{-2}. (*d*) Compressional strain rate, 10^{-15} s^{-1}; Q_0 70 mW m^{-2}.

peak Moho temperature being 810 °C in figure 6*c* and 940 °C in figure 6*d*; this range is considerably smaller than the range of 460–830 °C that is calculated for the case where exhumation is accomplished by erosion (England & Thompson 1984, figure 5*d*,*f*).

3.3.3. *Post-collisional lithospheric strength*

Figure 7 shows the variation of the force per unit length required to maintain deformation, and of the depth to the brittle–plastic transition during strain, first for cases in which the initial surface heat flow, Q_0, is 60 mW m^{-2} and the compressional strain rates are 3×10^{-16} s^{-1}, 10^{-15} s^{-1}, 3×10^{-15} s^{-1} and 10^{-14} s^{-1} (figure 6 *a*,*c*) and secondly for the cases in which the compressional strain rate is fixed at 10^{-15} s^{-1}, and Q_0 varies from 40–70 mW m^{-2}. The values of these quantities during the compressional phase have already been shown in figures 3 and 4; here they are plotted against time. Because it is assumed that no extensional strain occurs until the Moho temperature reaches 750 °C, the lithospheric strength and depth to the brittle–plastic transition are undefined between the end of compression and the onset of extension. The driving stress at the onset of extension is close to 4×10^{12} N m^{-1} in all cases (see

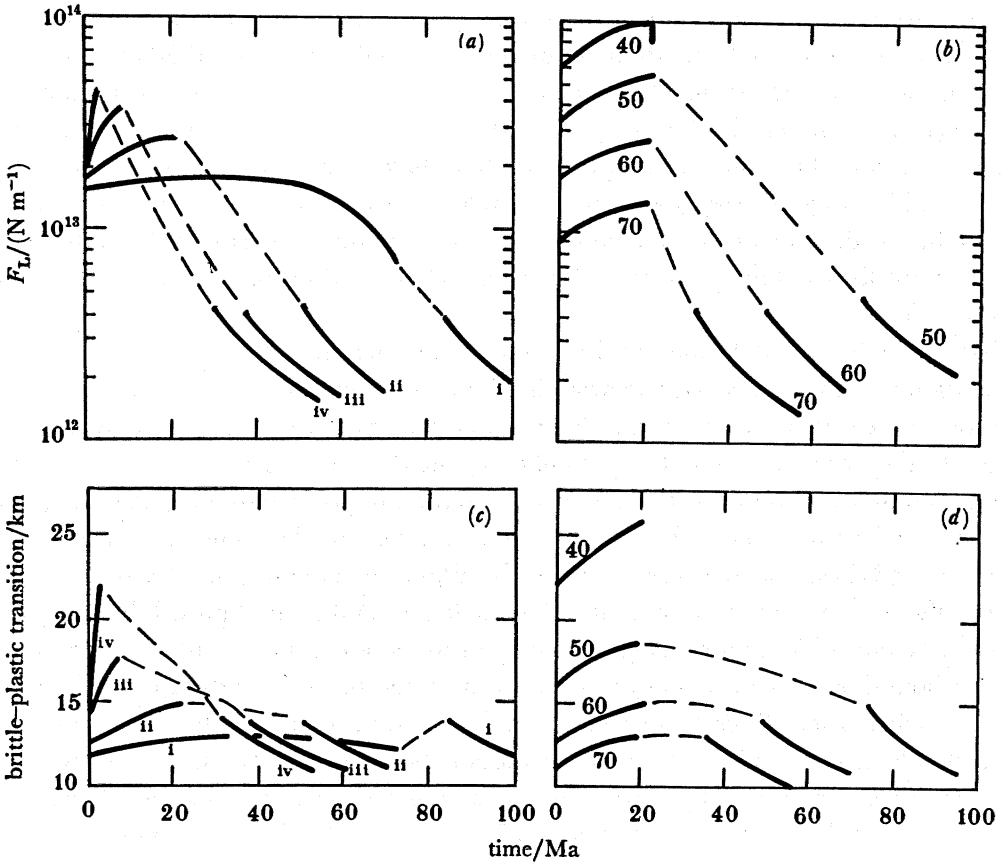

FIGURE 7. Evolution of F_L and the depth to the brittle–plastic transition with strain for lithosphere of rheological and thermal parameters given in tables 1 and 3. In each case a homogeneous compressional strain of $\gamma = 2$ is followed by an interval of no strain; once the Moho temperature exceeds 750 °C there is homogeneous extensional strain of 100% at 10^{-15} s^{-1} (see text).

(*a*), (*c*) Q_0 is 60 mW m^{-2} and compressional strain rates are 3×10^{-16} (curves (i), 10^{-15} (ii), 3×10^{-16} (iii) and 10^{-14} s^{-1} (iv)). Compressional strain rate is 10^{-15} s^{-1} and the values of Q_0 in mW m^{-2} are given by each curve.

figure 4) and it drops in rough proportion to the strain, as would be expected for isothermal extension (see, for example, England 1983*a*; Houseman & England 1986*a*). There is little variation in the calculated depth of the brittle–plastic transition at the onset of extension (between 13 and 16 km) and this, too, is attributable to the similarity of geotherms at the onset of extension (see figure 6). The timescale for diffusion of heat through the upper crust is sufficiently short for there to be appreciable cooling of these levels during extension, and consequently the brittle–plastic transition does not decrease in depth in proportion to the extensional strain.

4. Discussion

4.1. *Tectonic evolution*

In this paper the continental lithosphere has been treated as a thin, continuous sheet whose rheology is described by the frictional and creep laws summarized in table 1. This treatment shows that the minimum width of deformation associated with a zone of continental convergence should be approximately $2W/(\pi\sqrt{n})$, where W is the along-strike length of the zone,

PHILOSOPHICAL TRANSACTIONS OF THE ROYAL SOCIETY A MATHEMATICAL, PHYSICAL & ENGINEERING SCIENCES

and n is the effective stress exponent of the integrated rheology; this relation probably does not hold for compressional belts less than about 1000 km long (see §2 and England *et al.* 1985).

The strain rates characteristic of the compressional deformation may be estimated by dividing the convergent velocity by the across-strike width of the deformation and, under the conditions in which the thin sheet approximation holds, fall in the range $10^{-14}\,s^{-1}$ to $3\times10^{-16}\,s^{-1}$. This range overlaps what is often referred to as the geological range of strain rates; the higher strain rates are great enough to ensure virtually isothermal deformation, while the time constant for the lowest strain rate is comparable to that for the thermal relaxation of the lithosphere.

The first stage in the deformation in a large continental collision zone involves the accommodation of convergence over an area that is about as wide as the compressional margin is long (above); the diffuse nature of this deformation does not arise from the buoyancy of the continental lithosphere but from the roughly exponential decay, with distance from the convergent boundary, of the stress associated with that boundary condition (§2.1; England & McKenzie 1982; England *et al.* 1985; Houseman & England 1986*b*). The analytical solutions (England *et al.* 1985) do not treat the problem of oblique convergence, but it is to be expected that when convergent motion is dominant, the scale length of deformation will be comparable to that of pure compression, whereas the convergent motion associated with a predominantly transcurrent boundary will probably be taken up over the shorter length appropriate to the transcurrent deformation. This theory makes no prediction as to which of two converging continents should accommodate the relative motion by deforming and, in principle, both should. In practice, there is usually a pronounced asymmetry in convergent belts. For example Eurasia appears to deform more rapidly than do India and Arabia in their respective collisions with Eurasia; and I accept Molnar & Tapponnier's (1981) suggestion that thermal contrasts may determine which of two colliding continents deforms (see §3.2 and figure 3).

If convergent deformation continues long enough, the buoyancy forces associated with isostatically compensated elevation contrasts become great enough to inhibit further thickening and to transfer the compressional deformation further away from the convergent boundary (Tapponnier & Molnar 1976). This stage of the orogeny is characterized by plateau-like topography and by the increasing prominence of strike-slip deformation; further deformation increases the area, but not the elevation, of the plateau (Houseman & England 1986*b*). The most prominent present example of such deformation is the Tibetan plateau, which exhibits strike-slip and extensional deformation, following a Tertiary history of crustal thickening (Molnar & Tapponnier 1975; Tapponnier & Molnar 1976, 1978; Molnar & Chen 1983). The buoyancy forces associated with the elevated plateau appear to be a prerequisite for the strike-slip deformation (Houseman & England 1986) and a simple mass balance calculation shows that the present Tibetan plateau accounts for most of the Tertiary convergence between India and Asia, despite the present predominance of strike slip deformation (England & Houseman 1986).

Deformation during this second stage represents the superposition of convergent deformation, which in the simplest case produces essentially biaxial strain, on a tendency for the elevated region to spread radially; in the India–Asia collision this combination leads to strike-slip and extensional faulting that reflect North–South shortening plus East–West extension (Tapponnier & Molnar 1976; Molnar & Chen 1983). Once convergence ceases, only the extensional strains will occur although, as discussed in §3.3.1, these rates may initially be much slower than the convergent strain rates were. The present East–West extensional strain rates in Tibet seem to

PHILOSOPHICAL TRANSACTIONS OF THE ROYAL SOCIETY A MATHEMATICAL, PHYSICAL & ENGINEERING SCIENCES

be about 2×10^{-16} s^{-1} (Molnar & Deng 1984); at this rate a strain of 100% would take 100 Ma. However, the continuing temperature increase in thickened continental crust can readily result in a decrease in strength of the lithosphere and a final stage of rapid extension. This appears to have been the case for the Basin and Range province of North America (see, for example, Molnar & Chen 1983).

4.2. *Rheological development*

Variation in strain rate does not appreciably affect the thermal structure of the belt during its compression unless the strain rate is below about 3×10^{-16} s^{-1}, when the time scale for a strain of 100% is similar to the time for thermal relaxation of the lithosphere. However, the strong dependence of the rheology on temperature means that the effective viscosity of the lithosphere is influenced by temperature changes during deformation unless strain rates are higher than 3×10^{-15} s^{-1} (figure 3). The process most strongly influenced by temperature changes during deformation is the post-compressional extension (see §3.3 and §4.3 below).

During compressional deformation, temperatures rise most rapidly in the upper crust, where the effect of radiogenic heating is strongest; consequently, even at the highest strain rates considered, the brittle–plastic transition does not get deeper in proportion to the total strain, while it may become shallower at strain rates less than about 10^{-15} s^{-1} (figure 4). Equally, during extension, heat can diffuse readily through the uppermost crust and the depth to the brittle–plastic transition does not decrease in proportion to the strain; the calculated range in depth to the brittle–plastic transition during extension is 10–16 km (figure 7). These calculations can be compared with the distribution of earthquakes in zones of active continental deformation. Large crustal earthquakes in zones of continental convergence appear to nucleate generally above 25 km, with occasional earthquakes down to 50 km; the maximum depth of crustal earthquakes under the Tibetan plateau is shallower than 15 km, and shallower than in most other zones of continental convergence; crustal seismicity in regions of continental extension is mostly shallower than 10–15 km (Chen & Molnar 1983).

The crust beneath Tibet has probably doubled in thickness over the last 45 Ma (see, for example, Molnar & Tapponnier 1975); this corresponds to a strain rate of *ca.* 5×10^{-16} s^{-1}, which is sufficiently slow (figure 7) for the brittle–plastic transformation to remain at approximately the same depth throughout deformation (figure 7; equation (11), §3.2.3). If the strain had occurred isothermally, the maximum depth of earthquake activity might be expected to be greater beneath Tibet than in convergent zones with thinner crust, and certainly to be greater than within continental crust that had stretched isothermally by an appreciable amount.

There are several uncertainties in interpreting the relation between calculated depths to the brittle–plastic transition and the maximum depths of seismicity in zones of continental deformation. It seems unlikely that the quartz flow law of table 1 adequately represents the deformation properties of the middle crust in all regions of continental extension; it is not even clear that a brittle–plastic transition calculated on the basis of *any* steady-state flow law should correspond to the transition between seismic and aseismic deformation. Any middle crustal rheology that has a comparable temperature dependence to that of the quartz law used here, and produces a brittle–plastic transition in undeformed crust at depths comparable to the range of maximum depth of seismic activity in continental interiors (Chen & Molnar 1983, table 4, figure 6) will probably exhibit a narrow range of depths to the brittle–plastic transition, similar to that shown in figure 7, during deformation.

PHILOSOPHICAL TRANSACTIONS OF THE ROYAL SOCIETY A MATHEMATICAL, PHYSICAL & ENGINEERING SCIENCES

4.3. *Post-compressional metamorphic development*

The width of a convergent belt may be important in determining its post-compressional evolution as, if erosion acts primarily around the edges of broad (several hundreds of kilometres wide) orogenic belts, it is likely that the main means of crustal thinning will be extension, as probably was the case for much of western North America in the Tertiary, and as seems to be occurring in Tibet at present. The requirement for appreciable extensional strain rates is mainly a condition on the strength of the lithosphere, which is expressed in this paper in terms of the temperature at the Moho; if this temperature exceeds 750 °C, the rheologically stratified lithosphere summarized in table 1 will strain at 10^{-15} s^{-1} or more, in response to an extensional force per unit length of 4×10^{12} N m^{-1} (figures 5 and 7). In nature, there is probably not a single value of Moho temperature at which appreciable extensional strain rates are achieved, owing to variations in lithology, in crustal contribution to the lithospheric strength, in the geothermal gradient and in the buoyancy force associated with the overthick crust. Nonetheless it seems likely that, because of the heavy temperature dependence of the strength of earth materials, the range of thermal conditions that permit extension of the continental crust in response to buoyancy forces of a few times 10^{12} N m^{-1} is quite narrow (see figure 5, and Houseman & England 1986*a*; Sonder *et al.* 1986*b*). The absolute values of temperature discussed in this section are subject to the usual uncertainties associated with extrapolating laboratory flow laws (for example, table 1) to geological conditions.

The metamorphism accompanying the tectonic events outlined in §3 and §4.1 is limited in its intensity by the thermal regime necessary for extension to begin. In contrast to the case in which erosion limits the metamorphic development, the maximum temperatures achieved in the crust are relatively insensitive to the initial thermal conditions (compare figure 6 and England & Thompson 1984, figures 3, 4 and 5). While metamorphic studies may be of little use in determining the thermal budget of such belts, the pressure–temperature paths calculated in figure 6 suggest a clear way of distinguishing between possible tectonic histories on the basis of apparent pressure–temperature paths followed by rocks in a given metamorphic belt; the last phase of the thermal evolution of the paths illustrated in figure 6 is a thermal relaxation towards the initial geotherms (curves *a*, figure 6), which ought to be represented by a phase of isobaric cooling over several hundreds of degrees. The pressure–temperature paths shown in figure 6 are calculated without erosion and, in order for any of the buried rocks to be observed, there would have to be a later phase of tectonic activity, or some erosion along with the extension.

It is frequently noted that metamorphic isograds appear to be disrupted by tectonic activity after the peak of metamorphism (see, for example, Harte & Dempster, this symposium; Thompson & Ridley, this symposium). Although the disruption may be due, in some cases, to a phase of deformation entirely separate from that producing the metamorphism, it is likely that the final stage in the deformation of large compressional belts is the superimposition of strike-slip, and even extensional, deformation on the earlier compressional deformation. Strike-slip and normal faults, and their ductile continuations at depth, will juxtapose regions of different metamorphic grade during and after the peak of metamorphism (see, for example, Jackson, this symposium).

The conclusions of this paper concerning the rates and scale lengths of compressional deformation are only applicable to the case in which the deformation is spread out over a width

considerably greater than the lithospheric thickness (see §2 and table 2), but narrower mountain belts are equally subject to the buoyancy forces that result from crustal thickening, and should extend once the appropriate geothermal conditions are achieved. As well as the clear examples of extension in the larger orogenic belts of the present day (Tapponnier & Molnar 1976; Dalmayrac & Molnar 1981; Burchfiel & Royden 1986) there is growing evidence of such extensional activity in narrower belts, for example in the Betic Cordillera (Platt *et al.* 1983), in the Western Alps (Platt & Lister 1983) and in the Eastern Alps (Selverstone 1985); post-compressional extension may be a more common phenomenon in orogenesis than has previously been realized.

It is a pleasure to acknowledge numerous discussions on metamorphism and tectonics with Greg Houseman, Dan McKenzie, Peter Molnar, Stephen Richardson, Leslie Sonder and Alan Thompson that have contributed to the ideas expressed in this paper. Ron Oxburgh and Marc Parmentier provided helpful reviews. This work was supported by NSF grant EAR 84-08352.

References

Albarede, F. 1976 *Bull. Soc. géol. Fr.* **18**, 1023–1032.
Bird, P. & Piper, K. 1980 *Phys. Earth Planet. Inter.* **21**, 158–175.
Brace, W. F. & Byerlee, J. D. 1970 *Science Wash.* **168**, 1573–1576.
Brace, W. F. & Kohlstedt, D. L. 1980 *J. geophys. Res.* **85**, 6248–6252.
Burchfiel, B. C. & Royden, L. H. 1986 *J. geol. Soc. Lond.* (In the press.)
Chen, W. P. & Molnar, P. 1983 *J. geophys. Res.* **88**, 4183–4214.
Coney, P. J. & Harms, T. A. 1984 *Geology* **12**, 550–554.
Dalmayrac, B. & Molnar, P. 1981 *Earth planet. Sci. Lett.* **55**, 473–481.
England, P. C. 1983*a* *J. geophys. Res.* **88**, 1145–1152.
England, P. C. 1983*b* In *Mountain building processes* (ed. K. J. Hsu), pp. 129–140. London: Academic Press.
England, P. C. & Houseman, G. A. 1985 *Nature, Lond.* **315**, 297–301.
England, P. C. & Houseman, G. A. 1986 *J. geophys. Res.* **91**, 3664–3676.
England, P. C., Houseman, G. A. & Sonder, L. S. 1985 *J. geophys. Res.* **90**, 3551–3557.
England, P. C. & McKenzie, D. P. 1982 *Geophys. Jl R. astr. Soc.* **70**, 292–321.
England, P. C. & McKenzie, D. P. 1983 *Geophys. Jl R. astr. Soc.* **73**, 523–532.
England, P. C. & Richardson, S. W. 1977 *J. geol. Soc. Lond.* **134**, 201–213.
England, P. C. & Thompson, A. B. 1984 *J. Petr.* **25**, 894–928.
Frank, F. C. 1972 In *Flow and fracture of rocks* (*Geophys. Monogr.* no. 16) (ed. H. C. Heard, I. Y. Burg, N. L. Carter & C. B. Rayleigh), pp. 285–292. Washington, D.C.: American Geophysical Union.
Goetze, C. 1978 *Phil. Trans. R. Soc. Lond.* A**288**, 99–119.
Houseman, G. A. & England, P. C. 1986*a* *J. geophys. Res.* **91**, 719–729.
Houseman, G. A. & England, P. C. 1986*b* *J. geophys. Res.* **91**, 3651–3663.
Isacks, B. L., Oliver, J. & Sykes, L. R. 1968 *J. geophys. Res.* **73**, 5855.
Jackson, J. A. & McKenzie, D. P. 1984 *Geophys. Jl R. astr. Soc.* **77**, 185–264.
Le Pichon, X. 1983 In *Mountain building processes* (ed. K. J. Hsu), pp. 201–213. London: Academic Press.
McKenzie, D. P. 1969 *Geophys. Jl R. astr. Soc.* **18**, 1–32.
McKenzie, D. P. 1972 *Geophys. Jl R. astr. Soc.* **30**, 109–185.
Molnar, P. & Chen, W.-P. 1983 *J. geophys. Res.* **88**, 1180–1196.
Molnar, P. & Deng, X. D. 1984 *J. geophys. Res.* **89**, 6203–6228.
Molnar, P. & Lyon-Caen, H. 1974 *Geol. Soc. Am. Spec. Pub.* (In the press.)
Molnar, P. & Tapponnier, P. 1975 *Science, Wash.* **189**, 419–428.
Molnar, P. & Tapponnier, P. 1978 *J. geophys. Res.* **83**, 5361.
Molnar, P. & Tapponnier, P. 1981 *Earth planet. Sci. Lett.* **52**, 107–114.
Platt, J. P., van den Eeckhout, B., Janzen, E., Konert, G., Simon, O. J. & Weijermars, R. 1983 *J. struct. Geol.* **5**, 519–538.
Platt, J. P. & Lister, G. S. 1985 *J. struct. Geol.* **7**, 19–36.
Richardson, S. W. & Powell, R. 1976 *Scott. J. Geol.* **12**, 237–268.
Selverstone, J. 1985 *Tectonics* **4**, 687–704.

PHILOSOPHICAL TRANSACTIONS OF THE ROYAL SOCIETY A MATHEMATICAL, PHYSICAL & ENGINEERING SCIENCES

Sonder, L. J. & England, P. C. 1986 *Earth planet. Sci. Lett.* **77**, 81–90.
Sonder, L. J., England, P. C. & Houseman, G. A. 1986*a* *J. geophys. Res.* **91**, 4797–4810.
Sonder, L. J., England, P. C., Wernicke, B. P. & Christiansen, R. L. 1986*b* *J. geol. Soc. Lond.* (In the press.)
Tapponnier, P. & Molnar, P. 1976 *Nature, Lond.* **264**, 319–324.
Tapponnier, P. & Molnar, P. 1977 *J. geophys. Res.* **82**, 2905–2928.
Tapponnier, P. & Molnar, P. 1979 *J. geophys. Res.* **84**, 3425–3459.
Vilotte, J. P., Daignières, M. & Madaraiga, R. 1982 *J. geophys. Res.* **87**, 10709–10728.
Vilotte, J. P., Daignières, M., Madaraiga, R. & Zienckiewicz, O. C. 1984 *Phys. Earth planet. Inter.* **36**, 236–259.

PHILOSOPHICAL TRANSACTIONS OF THE ROYAL SOCIETY A MATHEMATICAL, PHYSICAL & ENGINEERING SCIENCES